ISSN 0145-8752, Moscow University Geology Bulletin, 2021, Vol. 76, No. 2, pp. 136–145. © Allerton Press, Inc., 2021.
Russian Text © The Author(s), 2021, published in Vestnik Moskovskogo Universiteta, Seriya 4: Geologiya, 2021, No. 1, pp. 31–41.

The Structure and Formation Conditions of the Campanian Deposits in the Northwest Caucasus (Galitsyno Section)

E. V. Yakovishina[a, *], L. F. Kopaevich[a], A. M. Nikishin[a], S. I. Freiman[a], and M. A. Ustinova[b]

[a] *Department of Geology, Moscow State University, Moscow, 119991 Russia*

[b] *Geological Institute, Russian Academy of Sciences, Moscow, 111017 Russia*

**e-mail: yakovishina@mail.ru*

Received May 12, 2020; revised June 30, 2020; accepted June 30, 2020

Abstract—Rocks in the Galitsyno quarry located in the Adler region of the North Caucasus are described. The quarry is of interest, because the excellent exposure in the relatively homogeneous carbonate rock sequence makes it possible to identify certain changes that reflect events that were common to the Late Cretaceous, in this case, the Late Campanian. These include the carbonate sedimentation characteristics of this geochronological interval, constant fluctuations in the relative sea level, and periodic volcanic activity. All these events are confirmed by the structural features of the section, various lithological rock types, as well as by the specific composition of microorganism complexes. The use of different methods in the analysis of the factual material makes these conclusions convincing.

Keywords: Northwest Caucasus, Galitsyno section, Campanian, Maastrichtian, carbonate sedimentation, clinoforms, nanoplankton, foraminifera, and volcanic activity

DOI: 10.3103/S0145875221020150

INTRODUCTION

Campanian deposits are a subject of constant interest of researchers for a number of reasons. First, the Campanian is the longest subdivision within the Late Cretaceous, of more than 11 Ma; second, it was marked by one of the most powerful transgressions that led to the formation of various carbonate rocks, including specific types such as writing chalk stone; third, very important events were recorded during the Campanian, for example, climate fluctuations. Its beginning and end were characterized by almost subglobal cooling (Beniamovsky et al., 2014; Huber et al., 2018; Kopaevich and Vishnevskaya, 2016; Petrizzo, 2000, 2002; Vishnevskaya and Kopaevich, 2020). Fourth, it was one of the most powerful impulses of volcanic activity, which left a mark in sections not only of the Crimea, but also the North Caucasus (Gavrilov et al., 2014, p. 526; Kopaevich and Khotylev, 2014; Nikishin et al., 2013). The cyclic structure of most Campanian sequences are indicative of sea level fluctuations. These data are also important to reconstruct the paleo-oceanologic settings. All these facts mean that any section of deposits of this age is interesting because it helps to expand the understanding of this very important Late Cretaceous interval. For this reason, the Galitsyno quarry section described in this paper attracted our attention.

MATERIALS AND METHODS

The outcrop is a northwestern wall of the limestone quarry located to the southeast of the Galitsyno Settlement (Adler region, Northwest Caucasus) (Fig. 1). The exposed part of the quarry has a size of 360 × 17 m. The major sequence is subhorizontal to monoclinal.

All types of analyses and the creation of thin sections were carried out at the Department of Geology, Moscow State University, except for the study of nanoplankton. The rock composition was studied in thin sections, which were sampled at different levels from carbonate and clayey differences. A total of 27 thin sections were studied. Five lithological rock types were identified in the course of the study of petrographic thin sections (Fig. 2). The clay mineralogical composition was studied by X-ray phase analysis of three samples using an ULTIMA-IV X-ray diffractometer.

Informative data on the rock age were obtained by the nanoplankton study. Thirty samples out of 40 that were processed contain coccoliths as a small number of moderately and poorly preserved specimens. Shells were identified by the standard method (Bown and Young, 1998) and were studied using a BiOptik light polarizing microscope at a magnification of 1000. Nanoplankton has a medium level of preservation in the studied limestones; many coccoliths are broken and bear secondary recrystallization traces. In the clayey interlayers, well-preserved coccoliths did not

Fig. 1. A map of the quarry near the Galitsyno Settlement.

undergo secondary changes. Photo images of the shells were made under a light microscope under crossed nicols and under MV 2300 WegaTescan SEM at the Geological Institute, Russian Academy of Sciences.

Foraminifera shells were studied in thin sections, because the rocks were relatively hard, except for two limestone samples that were soft enough to extract shells of planktonic (PF) and benthic (BF) foraminifera, as well as clay interlayers from members 1 and 2. Foraminifera shells, mainly planktonic, were found in all thin sections; however, not all of them could be identified to the species level. Images of major age determination taxa were shown and their stratigraphic distribution was indicated. The PF and BF index species were photographed using Tescan 2300 SEM in the BSE detector mode at the Geological Institute, Russian Academy of Sciences, and JEOL JSM-6480LV EM at the Department of Geology, Moscow State University.

Section description. The section is composed of similar grey medium- and fine-layered limestones with numerous stylolite seams and parallel bedding. The central part of the quarry wall is marked by a range of ruptures with a small fault propagation fold along clays at the top of the “clinoform” member.

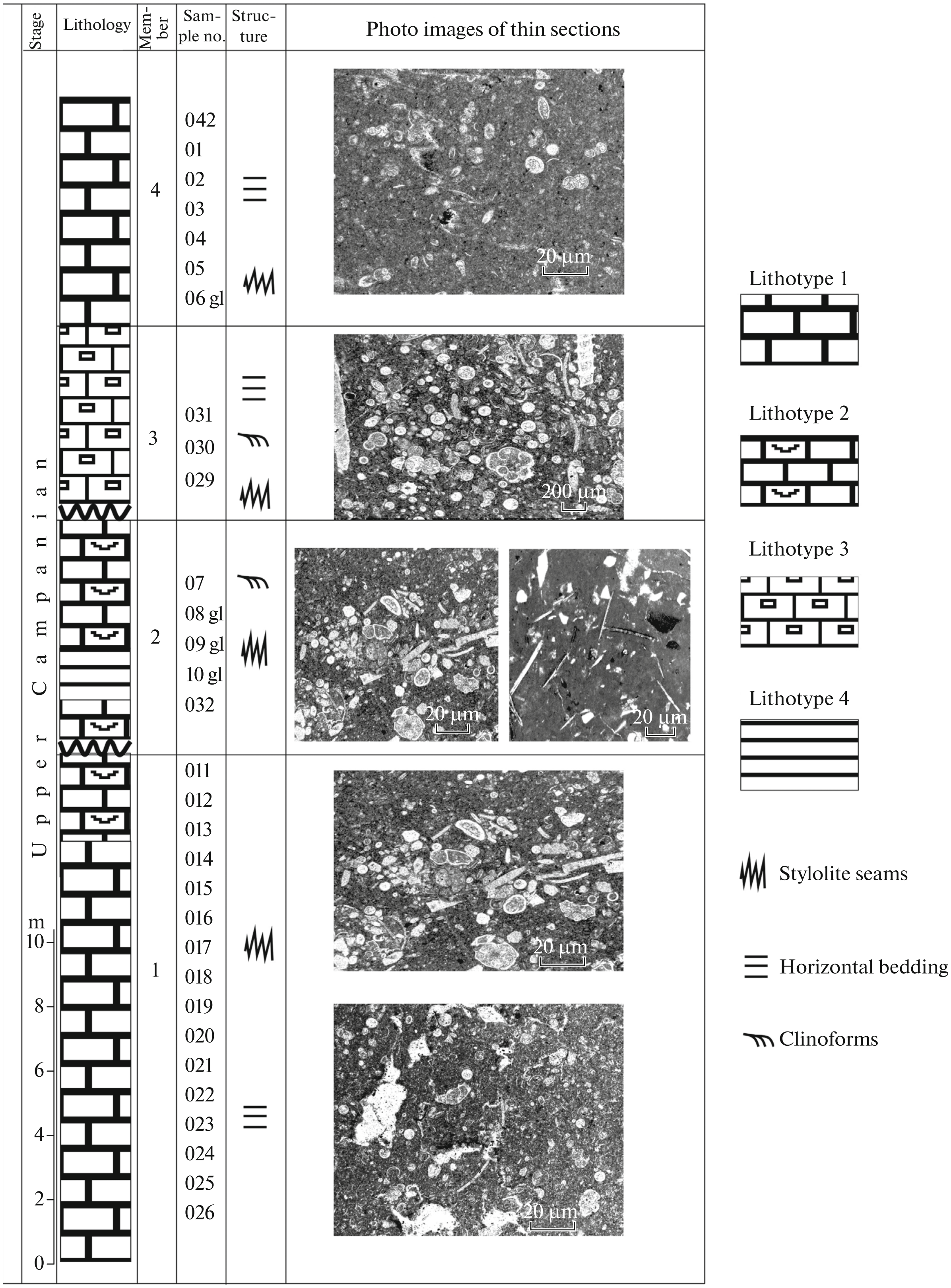

Fig. 2. The stratigraphic column and lithological types of the Galitsyno section: lithotype 1, micritic limestone (wackestone), organic fragmental, samples nos. 01, 03, 04, 019, 023, 027, 031, and 032; lithotype 2, organic fragmental limestone (wackestone–packstone), foraminiferal, samples nos. 02, 05, 011, 014, 016, 017, 018, 020, 021, 025, 026, 030, and 041; lithotype 3, organic fragmental limestone (wackestone–packstone), calcispheric, samples nos. 07, 012, 015, 029, and 040; lithotype 4, calcareous clays (%): montmorillonite (56), feldspars (8), micas (muscovite and phlogopite) (12), calcite (3), quartz (1), and amorphous substance (volcanic glass (?), 20), samples nos. 08, 09.

Stage	Preservation	Sample no.	*Ahmuerella octoradiata*	*Arkhangelskiella cymbiformis*	*Biscutum ellipticum*	*Biscutum magnum*	*Braarudosphaera bigelowii*	*Braarudosphaera discula*	*Broinsonia parca constricta*	*Calculites* sp.	*Chiastozygus litterarius*	*Chiastozygis* sp.	*Cribrosphaerella ehrenbergii*	*Ceratolithoides aculeus*	*Cretarhabdus crenulalus*	*Cyclagelosphaera deflandrei*	*Cyclagelosphaera margerelii*	*Cylindrathus serratus*	*Eiffellithus turriseifeli*	*Manivitella pemmatoidea*	*Manivitella* sp.	*Micula concava*	*Micula decussata*	*Micula praemurus*	*Microrhabdulus decoratus*	*Orastrum* sp.	*Placozygus fibuliformis*	*Prediscosphaera cretacea*	*Prediscosphaera grandis*	*Quadrium gartneri*	*Rhagodiscus angustus*	*Uniplanaruis gothicus*	*Uniplanaruis sissinghii*	*Zeugrhabdotus diplogrammus*	*Watznaueria bamesae*	*Watznaueria biporta*	*Watznaueria fossacincta*	*Watznaueria manivitae*
Upper Campanian–lower Maastrichtian	M	1		VR						S					S		S						R		S		S					S			R	VR	S	
	M	2		VR											S		F						R	S	F							S			F	F	F	R
	M	3		VR											S		F						R		R		VR				VR				F	R	R	F
	M	4															VR		S				R		S		S					R			F	R		
	M	5		VR					VR						VR	VR	F		VR				R		R	S	VR					F			F	R	S	
	G	6	S																																R			
	M	7				S			VR	VR						VR	F						R		R		S					R			F		F	
	G	8															VR								R										VR			
	G	8/2													S								R									S	S		F		S	
	G	9	S		VR	R	VR					S	VR	S	VR			S		VR		S			F		VR	VR	S		S	S		VR	F	S	F	VR
	G	9/2	S	S	VR	VR					S		VR	VR			VR		S	VR	VR	S	VR		F		S		S	S		S		VR	F	S		
	G	9/3		VR		VR	VR	VR	VR			S	VR	VR	VR		S		S	VR		F	VR		R	S	S				S	VR		VR	F	VR	F	S
		10																																				
	G	10/2			VR	S											VR				VR				F						S	S			F		VR	
	M	11											S				F						S		VR		S			S					F	VR	F	VR
	M	12				VR			S							S	F										VR					VR			F	VR	VR	
	M	13	S	S			VR		S					S	S			S		S	VR	F	R	S		S						VR	VR		VR	VR	S	
	M	14				S				S							F		VR			S				S	S				S	R			F		F	
	M	15														S	F	S					S		S							VR			F	F	R	
	M	16		VR		VR			S								F		R				VR		VR	S				S		S			F	R	R	VR
	M	17							S								F						VR				S								F	R	F	F
	M	18	VR		S	VR				VR							F			VR		S									S	VR			F		R	
	M	19		S		S			VR	VR					VR	VR	F		R				VR		S	VR	VR			S	S	S			F	F	R	
	M	20														VR	VR		R				VR				S								F	F	F	R
	M	21			S				S					S	S	VR	VR		R																F	F	F	F
	G	22															VR					VR													S		S	
	M	23					S							S		VR	VR		S	VR		VR	VR			VR	VR					R	S		F	F	R	
	G	24												S			VR					F	VR							S		F	F		VR		F	
	M	25												S			VR																		F	F	F	F
	M	26							S							S	F		VR						S		S					R			F	F	F	F
	M	27	S		S									S			F		VR								VR								F	F	F	F
	G	28																		VR		F	VR	S									R		F		R	
	M	29			S									S			F		S			VR	S		S							F			F	F	F	R
	M	30			S									S		VR	F		S	VR		VR	S							S	S	F			F	F	F	VR
	M	31		S					VR					VR		VR	F		S				S		S	S				S		F			F	F	F	
	M	32														VR	F									VR						F			F	R	R	
	M	40		S						S					VR	VR	F					F			R		S				VR	F			F	S		
	G	41						VR									S				VR		VR												R			
	M	42		S					VR					S	S		F		VR			VR			F	VR						R			F	R	VR	
	M	43		S					S													VR			F							S			F	R	S	

Fig. 3. The calcareous nanoplankton distribution in the Galitsyno section. The relative contents of calcareous nanoplankton: few (F), 1–5 specimens per 10–20 fields of view; rare (R), 1 specimen per 100 fields of view; very rare (VR), 1 specimen for 200 fields of view; and sporadic (S), 1–2 specimens for the entire sample. Preservation: M (medium), coccoliths are partially dissolved and recrystallized; G (good), coccoliths remained unchanged.

Member 1. The section bottom is composed of thick-bedded limestones with black siliceous nodules (Fig. 2). Limestones are massive, compact, light beige, with a shell-like fracture and many stylolite seams, interbedded with darker differences and relatively softer varieties. Three grey plastic clay interlayers of 2–6 cm thick were found. The member is 15-m thick (Fig. 2). The first member is characterized by interlayering of lithological type 1 and 2 limestones; calcispheric limestones can be found in the roof (lithotype 3).

Member 2 overlies the member 1 with a sharp erosional contact with a distinct clinoform structure. The cut depth reaches 6.5 m in some areas. The member is composed of monoclinal whitish beige, thick-to-medium-bedded limestones with ferruginization along the cracks and numerous stylolite seams. Ferruginization as spots developed after limestones of this member. Three clay interlayers, 5-, 10-, and 17-cm thick, respectively, were found in the roof. Clays are brown to greenish grey, plastic, with carbonate material interlayers. Bedding angles vary greatly within the member and range from 5 to 40°; the dip azimuth is 190–235° SW. Inside the member are two erosion boundaries cutting layers with different bedding angles. Two oval olistolith bodies of 1.5 × 0.8 m, composed of grey massive rounded limestones, were found within this member in the northern part of the quarry's northwestern wall. The thickness of the member ranges from 0 to 6.5 m. The member contains organic–detrital limestones (lithological type 4) (Fig. 2). According to the X-ray phase analysis results, clays contain the following minerals (%): montmorillonite (56), feldspar (8) (albite (2), microcline (10)), mica (muscovite, phlogopite, 12), calcite (3), quartz (1), and amorphous substance (volcanic glass, 20).

Member 3. Medium–fine-layered grey limestones with stylolite seams parallel to the bedding occur on the underlying member with erosion contact. Very thin clay interlayers (up to 1 mm) are rare. According to the studied petrographic thin sections from the member, the rocks mainly include calcispheric limestones (lithological type 3) (Fig. 2). The thickness of the member is from 0 to 2.3 m.

Member 4 overlies the underlying member conformably. Limestones are medium–fine-layered, compact, massive, light beige, with a shell-like fracture and stylolite seams parallel to the bedding. In member 4 the deposits are mainly composed of foraminifera limestones (lithotypes 1 and 2).

RESULTS AND DISCUSSION

Lithological types. The study of thin sections made it possible to identify four lithological types, which in terms of formation conditions can be attributed to several facies zones (Flugel, 2010). Lithological types 1, 2 (member 1) refer to the FZ2 facies zone (nerite, open sea) which is characterized by normal salinity, oxygen saturation, and calm hydrodynamic setting. Lithological types 3, 4 (member 2) refer to the FZ3 facies zone (slope bottom) which is characterized by normal salinity and oxygen conditions, and active hydrodynamic environment; deposits are often brecciated. According to the X-ray phase analysis, clay interlayers were formed along ash interlayers. These interlayers are explained by the influence of a large volcanic belt that stretched from the Eastern Pontids to the Lesser Caucasus (Afanasenkov et al., 2007; Barrier and Vrielynck, 2008; Nikishin et al., 2003, 2013; Okay et al., 1997; Rolland et al., 2010).

Hence, it can be assumed that member 1 was formed on the open shelf in a calm hydrodynamic setting. The boundary between members 1 and 2 was marked by more active hydrodynamic conditions and by a partial erosion of earlier accumulated deposits resulted in the development of erosive landforms. These processes were most likely due to a greater tectonic activity, as indirectly indicated by clays formed along the ash interlayers. Subsequently, clinoforms filling the erosional cuts can be noted in member 2. The visible size of these cuts is up to 5–6 m. The boundary between the members corresponds to the paleorelief at the maximum cut moment.

Fig 4. Photo images of calcareous nanoplankton from the Galitsyno section under a light microscope with crossed nicols: (*1*) *Ahmuerella octoradiata* (Górka, 1957) Reinhardt, 1966, sample 9; (*2*) *Chiastozygus* sp., sample 9; (*3*) *Zeugrhabdotus diplogrammus* (Deflandre in Deflandre and Fert, 1954) Burnett in Gale et al., 1996, sample 9/2; (*4*) *Placozygus fibuliformis* (Reinhardt, 1964) Hofmann, sample 3; (*5*) *Eiffellithus turriseiffelii* (Deflandre in Deflandre and Fert, 1954) Reinhardt, 1965, sample 9/2; (*6*) *Cylindralithus serratus* Bramlett and Martini, 1964, sample 13; (*7*, *8*) *Cribrosphaerella ehrenbergii* (Arkhangelsky, 1912) Deflandre in Piveteau, 1952, sample 9 ((*7*) in transmission, (*8*) crossed nicols); (*9*) *Biscutum ellipticum* (Górka, 1957) Grun in Grun and Allemann, 1975, sample 9; (*10*) *Cretarhabdus crenulatus* Bramlett et Martini, 1964, sample 9; (*11*) *Prediscosphaera cretacea* (Arkhangelsky, 1912) Gartner, 1968, sample 9; (*12*) *Prediscosphaera grandis* Perch–Nielsen, 1979a, sample 9; (*13*) *Manivitella pemmatoidea* (Deflandre in Manivit, 1965) Thierstein, 1971, sample 13; (*14*) *Cyclagelosphaera margerelii* No. 1, 1965, sample 3; (*15*) *Cyclagelosphaera deflandrei* (Manivit, 1966) Roth, 1973, sample 19; (*16*) *Watznaueria barnesiae* (Black, 1959) Perch–Nielsen, 1968, distal side, sample 3; (*17*) *Watznaueria fossacincta* (Black, 1971a) Bown in Bown and Cooper, 1989a, sample 17; (*18*) *Watznaueria biporta Bukry*, 1969, sample 3; (*19*) *Watznaueria manivitae* Bukry, 1973d, sample 17; (*20*, *21*) *Arkhangelskiella cymbiformis* Vekshina, 1959 ((*20*) sample 3, (*21*) sample 9); (*22*) *Broinsonia parka constricta* Hattner, Wind et Wise, 1980, sample 9/3; (*23*) *Orastrum* sp., sample 3; (*24*) *Braarudosphaera bigelowii* (Gran and Braarud, 1935) Deflandre, 1947a, sample 9; (*25*) *Micula decussata* Vekshina, 1959, sample 3; (*26*) *Micula concava* (Stradner in Martini and Stradner, 1960) Verbeek, 1976b, sample 13; (*27*) *Uniplanarius gothicus* (Deflandre, 1959) Hattner and Wise, 1980, sample 5; (*28*) *Uniplanarius sissinghii* Perch–Nielsen, 1986b, sample 13; (*29*) *Microrhabdulus decorates* Deflandre, 1959, sample 9; (*30*) *Ceratolithoides aculeus* (Stradner, 1961) Prins and Sissingh in Sissingh, 1977, sample 9/2.

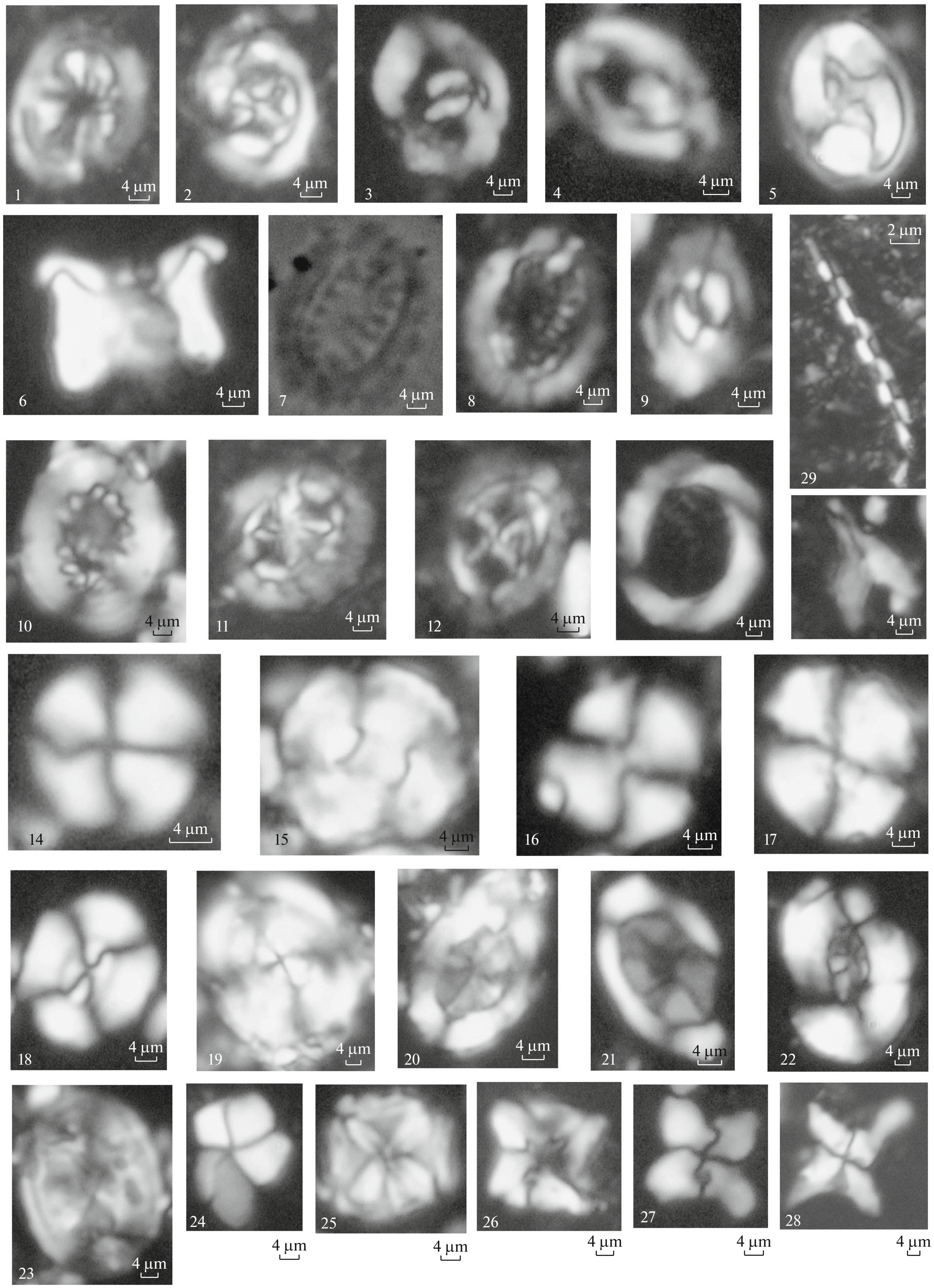
1
4 μm
2
4 μm
3
4 μm
4
4 μm
5
4 μm
6
4 μm
7
4 μm
8
4 μm
9
4 μm
2 μm
29
10
4 μm
11
4 μm
12
4 μm
4 μm
4 μm
14
4 μm
15
4 μm
16
4 μm
17
4 μm
18
4 μm
19
4 μm
20
4 μm
21
4 μm
22
4 μm
23
4 μm
24
4 μm
25
4 μm
26
4 μm
27
4 μm
28
4 μm

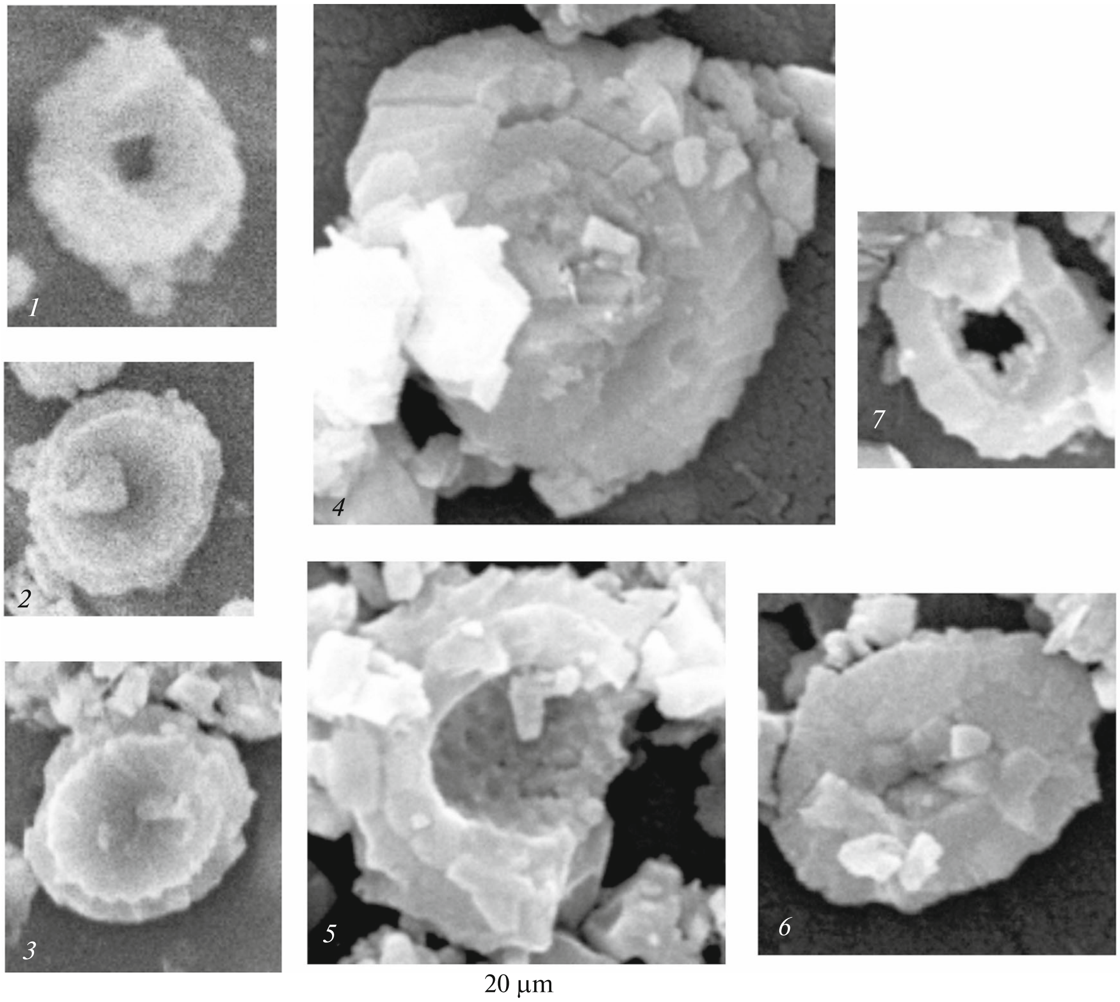

Fig. 5. Photo images of nanofossils under a scanning microscope: (*1*) *Cyclagelosphaera margerelii* Noël, 1965, proximal side, sample 3; (*2*) *Watznaueria barnesae* (Black, 1959) Perch–Nielsen, 1968, proximal side, sample 9; (*3*) *Watznaueiia fossacincta* (Black, 1971a) Bown in Bown and Cooper, 1989a, proximal side, sample 9; (*4*) *Watznaueria manivitae* Bukry, 1973d, distal side, sample 9; (*5*) *Arkhangelskiella cymbiformis* Vekshina, 1959, proximal side, sample 9; (*6*) *Biscutum ellipticum* (Górka, 1957) Grun in Grun and Allemann, 1975, distal side, sample 9; (*7*) *Seribiscutum* (?) sp., distal side, sample 42.

The deposits composed of organic–detrital limestones correspond to the sea-level-drop stage. Some paleobottom protrusions with a similar morphology take the form of erosion boundary: the northeastern slope is gentle and the southwestern edge is steep. This form can be indicative of a southwestern current direction. The stream actively washed away the northeastern slope and smoothed the southwestern slope, during flow down from it. Sedimentation at that time was conformable to the paleorelief. Massive poorly layered members were accumulated on the side of the steep slope, whereas the gently sloping part was characterized by accumulation of the clinoform member with SW orientation of its individual components.

In terms of their composition, clays were related to the periodic volcanic activity. Three clay interlayers with a thickness of 7 to 15 cm are cut erosively by the overlying sediments. They can be found in three areas that are abruptly isolated by the erosion boundary. The sequences of the high sea level most likely cut off at the third stage were not represented in the section. The following clinoform member was identified in member 3. Repeated cutting affected both the first- and the second-stage rocks. The apparent size of the cut reaches 4–5 m. At the macrolevel, the third-stage deposits consist mainly of calcispheric limestones; the material to form the member was brought in from the shallower part of the shelf. The likely reasons included a relative sea level drop and more active basin hydrodynamics. The clinoform member groundmass was likely accumulated at that time. One more erosion boundary can be traced in the member itself.

The fourth stage (member 4) was characterized by relatively uniform erosion: smoothing of bottom irregularities without visible cutting. Member 4 is composed largely of foraminifera limestones, mudstones with a shell-like

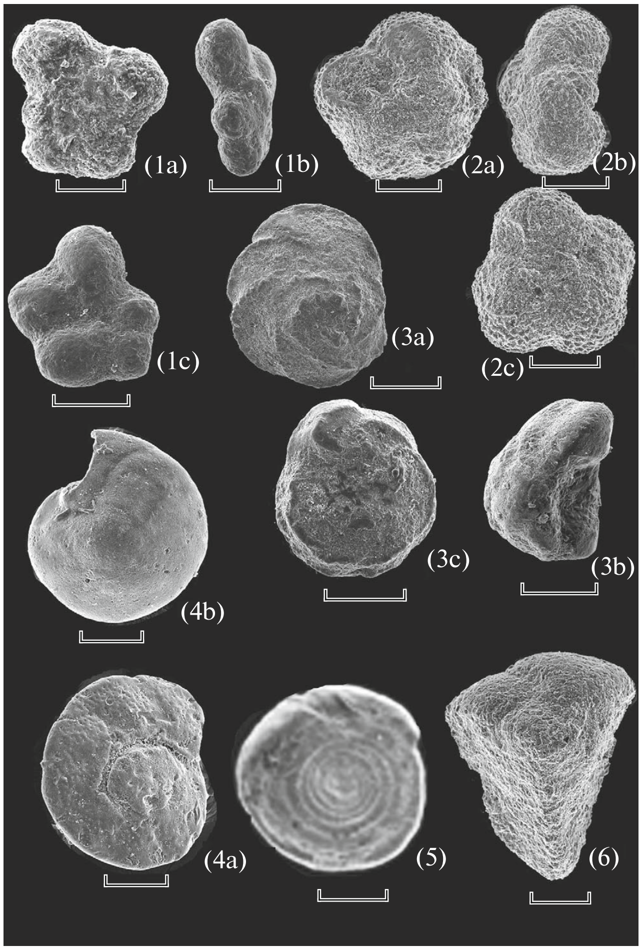

Fig. 6. Photo images of planktonic and benthic foraminifera under a scanning microscope. In Figs. 6 and 7, for conispiral shells: (a) dorsal view, (b) lateral view, (c) umbilical view; scale bar, 200 µm. (1a–1c) *Globotruncanella petaloidea* (Gandolfi, 1955), sample 9; (2a–2c) *Rugoglobigerina rugosa* (Plummer), sample 5; (3a–3c) *Contusotruncana morozovae* (Vasilenko,1961), sample 5; (4a, 4c) *Cibicidoides voltzianus* (d'Orbigny, 1840), sample 32; (5) *Ammodiscus incertus* Reuss., sample 5; (6) *Gaudryina pyramidata* (Cushman, 1926), sample 5.

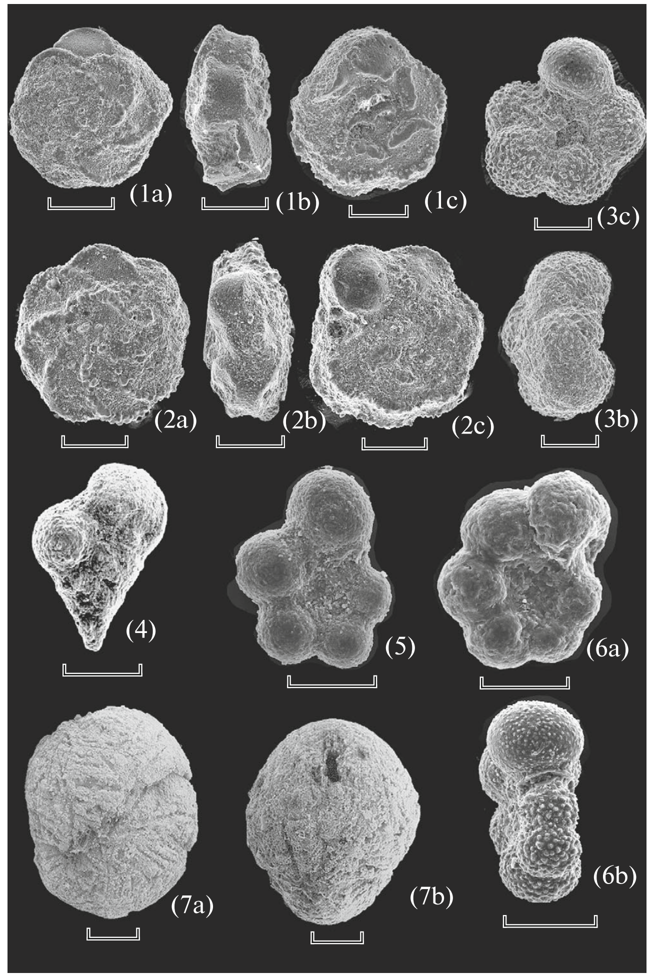

Fig. 7. Photo images of planktonic and benthic foraminifera under a scanning microscope: (1a–1c) *Globotruncana bulloides* Vogler, 1941, sample 9; (2a–2c) *Globotruncana arca* (Cushman, 1926), sample 026; (3b–3c) *Archaeoglobigerina australis* Huber, 1991, sample 1; (4) *Laeviheterohelix* cf. *glabrans* (Cushman, 1928), sample 5; (5) *Globigerinelloides volutus* White, 1928, sample 32; (6a–6b) *Globigerinelloides asper* (Ehrenberg, 1854), sample 32; (7a–7b) *Orbignyna ovata* (von Hagenow, 1942), sample 9.

fracture and many stylolite seams. It is likely that the basin was deepening and the hydrodynamic regimen was also changing at that time. Above, the deposits are already horizontal in bedding. They are composed of light grey layered limestones and mudstones with desquamation. The member 4 deposits were accumulated in relatively deep-water conditions similar to those of member 1.

A Biostratigraphic Description of the Section

Calcareous nanoplankton. Since nanoplankton was not numerous, its relative amount was determined as follows: few (F), 1–5 specimens per 10–20 fields of view; rare (R), 1 specimen per 100 fields of view; very rare (VR), 1 specimen for 200 fields of view; and sporadic (S), 1–2 specimens for the entire sample (Fig. 3).

Nanoplankton is unevenly distributed throughout the section. The most common species throughout the section include (Figs. 4, 5) *Watznaueria barnesiae* (Black, 1959); *W. biporta* Bukry, 1969, *W. fossacincta* (Black, 1971), *Microrhabdulus decoratus* Deflandre, 1959, few specimens of *Cretarhabdus crenulatus* Bramlett et Martini, 1964; *Arkhangelskiella cymbiformis* Vekshina, 1959; *Placozygus fibuliformis* (Reinhardt, 1964) Hofmann, 1970; *Uniplanarius gothicus* (Deflandre, 1959); *Broinsonia parka constricta* Hattner, Wind et Wise, 1980; *Eiffellithus turriseiffelii* (Deflandre in Deflandre and Fert, 1954); *Micula concava* (Stradner in Martini and Stradner, 1960); and *M. stauropora* Vekshina, 1959, etc. Only clayey differences contain *Zeugrhabdotus diplogrammus* (Deflandre in Deflandre and Fert, 1954), *Ceratolithoides aculeus* (Stradner,

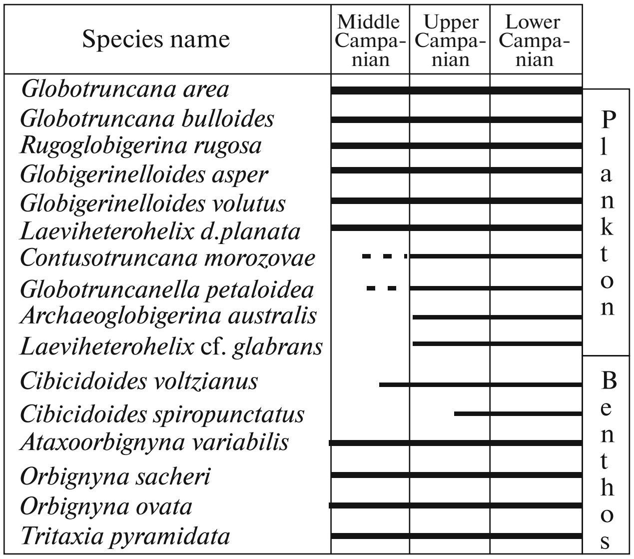

Fig. 8. The stratigraphic distribution range of foraminifera in the middle–upper Campanian and lower Maastrichtian deposits.

1961), *Cribrosphaerella ehrenbergerii* (Arkhangelsky, 1912), *Ahmuerella octoradiata* (Gorka, 1957), *Prediscosphaera cretacea* (Arkhangelsky, 1912), *Pr. grandis* Perch–Nielsen, 1979a, and *Chiastozygus* sp.

The Campanian–Maastrichtian contains *Biscutum ellipticum* (Górka, 1957); *B. magnum* Wind and Wise in Wise and Wind, 1977; *Cylindratus serratus* Bramlett and Martini, 1964; and *Arkhangelskiella cymbiformis* (Ovechkina, 2007). The following taxa are distinguished by a more limited stratigraphic distribution: *Broinsonia parca constricta* (upper Campanian–Maastrichtian), *Uniplanarius gothicus* (Campanian–lower Maastrichtian), and *U. sissinghii* Perch–Nielsen, 1986 (upper Campanian–lower Maastrichtian). These three species, albeit in small numbers, make it possible to estimate the age of the host deposits at the late Campanian–early Maastrichtian (Kilasoniya, 1991; Bown, 1998). Other taxa have a wide distribution range from the Cenomanian to the Maastrichtian, inclusive. Regarding the nanoplankton habitat, the species such as *Ahmuerella octoradiata*, *Arkhangelskiella cymbiformis*, *Broinsonia parca constricta*, and *Eiffellithus turriseiffeli* suggest a relatively low temperature of surface waters (Ovechkina, 2007).

Foraminifera. Foraminifera shells were found in almost all samples studied. Their number, preservation degree, and unbroken shells/fragments vary. In general, most rocks are represented by planktonic foraminifera limestones. The rocks are hard, and the low-pressure washing results are subtle. The layer 3 samples contain agglutinating benthic foraminifers *Ataxoorbignyna variabilis* (d'Orbigny, 1840), *Orbignyna ovata* (von Hagenow, 1942), *O. sacheri* (Reuss, 1845), *Gaudryina pyramidata* (Cushman, 1926), *Ataxophragmium* sp., and *Ammodiscus* sp. Shells of the calcareous secretion BF and PF were extracted from clayey interlayers of layers 1 and 2 at their border with limestones. Secretion BF occur as *Cibicidoides voltzianus* (d'Orbigny, 1840) and *C. spiropunctatus* (Galloway et Morrey, 1931).

Planktonic foraminifera are represented by the shells of *Globotruncana arca* (Cushman, 1926); *G. bulloides* (Vogler, 1941); *Contusotruncana morozovae* (Vassilenko, 1961); *Globotruncanella petaloidea* (Gandolfi, 1955); *Rugoglobigerina rugosa* (Plummer, 1927); *Archaeoglobigerina australis* Huber, 1991; *Globigerinelloides asper* (Ehrenberg, 1854); and *G. volutus* White, 1928 (Figs. 6, 7). The listed taxa belong to conispiral and planispiral shells. In addition, there are spiral helix shells from the heterohelicide group. Their accurate species identification is impossible, because the shells of the one species are not well preserved and the shell sculpture is poorly visible, while the other species was identified with the use of thin sections. However, *Leviheterohelix* cf. *glabrans* (Cushman, 1928) and *L.* cf. *planata* (Cushman, 1928) can be assumed based on the location and increasing chambers in the whorl. Findings of the aforementioned calcareous secretion BF and PF make it possible to estimate the age of host deposits at the Late Campanian (Fig. 8). It was not possible to identify the typical Maastrichtian forms in this area, although spiral convex shells found in thin sections resembled the species *Contusotruncana contusa* (Cushman, 1926); this species can be found mainly in the Maastrichtian deposits. However, its accurate identification is doubtful, while all other forms were found in both Campanian and Maastrichtian deposits. The agglutinating benthic taxa with a wider stratigraphic distribution range in this area are also in agreement with a late Campanian and early Maastrichtian rock age.

CONCLUSIONS

The deposits of the Galitsyno section were formed in the late Campanian–early Maastrichtian. This has been confirmed in terms of nanofossils, as well as planktonic and benthic foraminifera complexes. Sediments were formed in the external shelf zone below the storm wave impact. Clays formed after the ash interlayers are indicative of periodic volcanic activity. In addition, the sea level decline stages are related to the formation of two members with clinoforms. The erosional cuts were caused by local tectonic movements at that time. Hence, all geological events that characterize the Campanian can be observed in the Galitsyno quarry section.

ACKNOWLEDGMENTS

We thank V.L. Kosorukov for constant assistance in obtaining and interpreting the X-ray phase analysis results. We are sincerely grateful to the employees of the Laboratory of Local Material Study Methods, Department of Geology, Moscow State University, for the possibility for constant joint work and obtaining the high-quality images of foraminifera shells. The valuable comments and the benevolence of the reviewers helped to improve this paper.

FUNDING

This work was supported by the Russian Foundation for Basic Research (projects nos. 18-05-00495 and 18-05-00503) and was carried out under the State Assignment of the Geological Institute, Russian Academy of Sciences (state registration nos. AAAA-A18-118021690155-7 and 0135-2019-0062).

REFERENCES

Afanasenkov, A.P., Nikishin, A.M., and Obukhov, A.N., *Geologicheskoe stroenie i uglevodorodnyi potentsial Vostochno-Chernomorskogo regiona* (Geological Structure and Hydrocarbon Potential of the East Black Sea Region), Moscow: Nauchn. Mir, 2007.

Barreir, E. and Vrielynck, B., *Paleotectonic Maps of the Middle East: Tectono-Sedimentary Palinspastic Maps from Late Norian to Piacenzian*, Com. Geol. Map World/UNESCO, 2008.

Beniamovsky, V.N., Alekseev, A.S., Podgaetskii, A.V., et al., Upper Campanian–Lower Maastrichtian sections of northern Rostov Oblast: Article 2. Depositional environments and paleogeography, *Stratigr. Geol. Correl.*, 2014, vol. 22, no. 5, pp. 518–537.

Bish, D.L. and Post, J.E., Quantitative mineralogical analysis using the Rietveld full-pattern fitting method, *Am. Miner.*, 1993, vol. 78, pp. 932–940.

Bown, P.R., *Calcareous Nannofossil Biostratigraphy*. London: Chapman and Hall, 1998.

Bown, P.R. and Cooper, M.K.E., Jurassic, in *Calcareous Nannofossil Biostratigraphy*, Cambridge: Kluwer Acad. Publ., 1998.

Flugel, Er., *Microfacies of Carbonate Rocks. Analysis, Interpretation and Application*, Berlin: Springer-Verlag, 2010.

Gavrilov, Yu.O., Shcherbinina, E.A., Golovanova, O.V., and Pokrovskii, B.G., Late Cenomanian paleoecological event (OAE 2) in the eastern Caucasus basin of Northern Peri-Tethys, *Lithol. Miner. Resour.*, 2013, vol. 48, no. 6, pp. 457–488.

Huber, B.T., Macleod, K.G., Watkins, D.K., and Coffin, M.F., The rise and fall of the Cretaceous hot greenhouse climate, *Global Planet. Change*, 2018, no. 167, pp. 1–23.

Kilasoniya, E.D., Late Cretaceous coccolithophorids from the Trialeti Ridhe and their stratigraphic significance, in *Tr. Akad. nauk Gruzii. Ser. N. Vyp. 107* (Trans. Georgian Acad. Sci. Ser. N. Vol. 107), Tbilisi: Metsniereba, 1991.

Kopaevich, L.F. and Khotylev, A.O., The stratigraphic setting of cretaceous volcanic rocks in Crimea and the North Caucasus, *Moscow Univ. Geol. Bull.*, 2014, vol. 69, no. 6, pp. 433–444.

Kopaevich, L. and Vishnevskaya, V., Cenomanian-Campanian (Late Cretaceous) planktonic assemblages of the Crimea–Caucasus area: Palaeoceanography, palaeoclimate and sea level changes, *Palaeogeogr., Palaeoclimat., Palaeoecol.*, 2016, vol. 441, pp. 493–515.

Krupskaya, V.V., Zakusin, S.V., and Shlykov, V.G., Determination of the mineral composition of soils by X-Ray diffractometry, *in Laboratornye raboty po gruntovedeniyu. Izd. 3-e, pererab. dopoln.* (Laboratory Workshop on Soil Science: A Training Manual (3ed ed., amend.)), Trofimov, V.T. and Korolev, V.A., Eds., Moscow, Vyssh. Sh., 2016.

Nikishin, A.M., Korotaev, M.V., Ershov, A.V., and Brunet, M.F., The Black Sea basin: Tectonic history and Neogene–Quaternary rapid subsidence modeling, *Sediment. Geol.*, 2003, vol. 156, nos. 1–4, pp. 149–168.

Nikishin, A.M., Ziegler, P.A., Bolotov, S.N., and Fokin, P.A., Late Palaeozoic to Cenozoic evolution of the Black Sea–Southern Eastern Europe region: A view from the Russian Platform, *Turk. J. Earth. Sci.*, 2011, vol. 20, pp. 571–634.

Nikishin, A.M., Khotylev, A.O., Bychkov, A.Yu., et al., Cretaceous volcanic belts and the evolution of the Black Sea Basin, *Moscow Univ. Geol. Bull.*, 2013, vol. 68, no. 3, pp. 141–154.

Okay, A.I. and Sahunturk, O., *Geology of the Eastern Pontides*, *AAPG Mem. Oklahoma, Tulsa: AAPG*, 1997, vol. 68, pp. 291–312.

Ovechkina, M.N., Calcareous nannoplankton of the Upper Cretaceous (Campanian and Maastrichtian) of the south and east of the Russian Platform, in *Tr. PIN RAN* (Trans. Paleontol. Inst. Russ. Akad. Sci.), Moscow: Nauka, 2007.

Petrizzo, M.R., Upper Turonian–Lower Campanian planktonic foraminifera from southern mid-high latitudes (Exmouth Plateau, NW Australia): Biostratigraphy and taxonomic notes, *Cretaceous Res.*, 2000, vol. 21, pp. 479–505.

Petrizzo, M.R., Palaeoceanographic and palaeoclimatic inferences from Late Cretaceous planktonic foraminiferal assemblages from the Exmouth Plateau (ODP Sites 762 and 763, eastern Indian Ocean), *Mar. Micropaleontol.*, 2002, vol. 45, pp. 117–150.

Pushcharovskii, D.Yu., *Rentgenografiya mineralov* (X-ray Analysis of Minerals), Moscow: Geoinformmark, 2000.

Rolland, Y., Sosson, M., Adamia, Sh., and Sadradze, N., Prolonged Variscan to Alpine history of an active Eurasian margin (Georgia, Armenia) revealed by $^{40}Ar/^{39}Ar$ dating, *Gondwana Res.*, 2010, vol. 20, pp. 798–815.

Vishnevskaya, V.S. and Kopaevich, L.F., Microfossil assemblages as key to reconstruct sea-level fluctuations, cooling episodes an palaeogeography: The Albian to Maastrichtian of Boreal and Peri-Tethyan Russia, in *Cretaceous Climate Eventsand Short-Term Sea-Level Changes. Spec. Publ.—Geol. Soc. London*, 2020, vol. 498, pp. 165–187.

Translated by E. Maslennikova